The Close Binary Fraction: A Bayesian Analysis of SDSS M Dwarf Spectra

ABSTRACT

I have used cross-correlation to determine radial velocities from 145,888 individual spectra of a magnitude-limited sample of 39,543 M dwarfs observed by the Sloan Digital Sky Survey (SDSS). I then used Bayesian analysis and Monte Carlo simulations to determine the close binary fraction of M dwarfs. While previous results on the close binary fraction were based upon very small samples and thus were unable to provide very precise values, the results that I present here are based on far larger samples, and are thus more precise and fit to serve as a constraint on proposed theories of star formation. After adjusting for my detection efficiency, I found the frequency of binary stars with $a < 0.4$ AU to be $3.0^{+.6}_{-.9}\%$. I also demonstrated that the close binary fraction, like the total binary fraction, decreases with decreasing primary mass.

The Close Binary Fraction: A Bayesian Analysis of SDSS M Dwarf Spectra

1 Introduction

A complete theory of star formation remains to be found and is a major open problem in astrophysics. Many theories have been proposed to explain star formation, but any successful theory must make predictions which agree with all of the relevant observations. In particular, in the special case of binary stars, star systems which consist of two stars orbiting their center of mass, the theory must yield conclusions which match the observational results. It follows that the frequency of binary stars determined by the theory must match those determined observationally or the theory can not possibly be correct. Thus, the observationally determined binary fraction can be used as a constraint on proposed theories of star formation.

Various investigations have examined the binary frequency for different spectral classes. Duquennoy & Mayor (1991) found that G stars have a binary frequency of $\sim$57%. Fischer & Marcy (1992) conducted a similar survey of early-M stars and found that they have a binary frequency of 42% $\pm$ 9%. As an intermediary result, based upon a sample of 62 objects, they also found that the frequency of binaries with 0.04 AU $< a < 0.4$ AU to be $\sim$1.8%. More recently, Allen (2007) found that ultracool dwarfs (M6 and later) have a binary frequency of 20% $\pm$ 4%. However, a common feature of all of these surveys is that they include a relatively small number of stars. Duquennoy & Mayor (1991) included 164 stars, Fischer & Marcy (1992) included 179 stars, and Allen (2007) included 361 stars. A survey which included a larger number of stars would be able to give more precise values for the binary frequency than the surveys that have been conducted so far.

In this paper, I shall address the close binary fraction rather than the total binary fraction. For this purpose, I have carried out an extensive investigation of M dwarfs (spectral classes M0-L0) observed by the Sloan Digital Sky Survey (SDSS) and used the tools of Bayesian analysis in order to determine the fraction of binaries with $a < 0.4$ AU.

2 Methods

The SDSS produced an unprecedented amount of spectroscopic data. Data Release 7 (DR7) includes spectra of over 1.6 million objects, 460,000 of which are stars. For each of these objects, a minimum of three 15 minute spectroscopic exposures were taken until certain requirements for the signal-to-noise ratio (S/N) were met (Abazajian et al. 2009). The sheer size of the data set and the fact that each object was observed several times are factors crucial to this analysis.

Before any analysis can occur, a list of stars observed by the SDSS of spectral classes M0-L0 is required. I used the clean list of M stars observed by the SDSS that was compiled by Knapp et al. (2010). Their list includes 51,193 stars of spectral classes M0-L0.

For each of the stars on this list, I wish to determine whether or not it is a binary star. I do this by looking for radial velocity (RV) variability. RV variability implies that a star is a binary, as a star that is not a binary has no forces acting upon its motion and thus continues to move at the same velocity so thus its radial velocity, the velocity of the star in the line of sight, is constant. On the other hand, the radial velocity of a binary star varies due to its orbit around the center of mass of the system. Before I can determine whether the star is undergoing RV variations, I must first determine its RV from each of several observations. The following procedure is used to determine the radial velocity.

2.1 Calculation of Radial Velocities

I determine the radial velocity of each observation of any object which satisfies the following conditions:

1. It is on the list compiled by Knapp et al. (2010),
2. the i magnitude of the object satisfies $16.00 \leq i \leq 20.50$, and
3. the time between the first and last observation, Δt, satisfies either 0 hr $\leq \Delta t \leq 4$ hr or 2 d $\leq \Delta t \leq 30$ d.

The reason for the two time selections is the following. If 0 hr $\leq \Delta t \leq 4$ hr, then the observations are close enough together in time that I would expect to see only a very small change in the radial velocity even if the object being observed is a binary star. Thus, the radial velocity variations observed among the objects which satisfy 0 hr $\leq \Delta t \leq 4$ hr are used to determine the accuracy of the radial velocity values that I calculate. On the other hand, among the set of objects with 2 d $\leq \Delta t \leq 30$ d, the time spread between the observations is long enough that if the object is a binary star it is possible that I would observe significant RV variations.

Due to the star's motion relative to Earth, the observed spectra is Doppler shifted relative to the spectra emitted by the star. By comparing the observed spectra to template spectra of a M star, it is possible to determine what value of the radial velocity results in the best fit between the template and the observed spectra. Obviously, in order to do this, it is necessary to have template spectra available against which to compare the spectra. Such template spectra are readily available. In this paper, I use the templates that Bochanski et al. (2007) produced for each of the spectral classes M0-L0 using over 4000 SDSS spectra.

Each observation is fitted to each of the 11 templates (one for each spectral class from M0-L0). Using a code written in Interactive Data Language (IDL), I determine the radial velocity that gives the best fit between the spectra and one of the templates by minimizing

$$\chi^2 = \sum_{i \in \mathrm{S}} [\frac{f_i - m(\lambda_i)}{\sigma_i}]^2 \tag{1}$$

where the sum is over all pixels in the set S (I return to the definition of the set S below), f_i is the flux of the i$^{\text{th}}$ pixel, $m(\lambda_i)$ is the value of the model at λ_i, the wavelength of the i$^{\text{th}}$ pixel, and σ_i is the standard deviation of f_i. For f_i, I used the spectra from the red arm of the SDSS spectrograph which spans the region $\lambda = 5800 - 9200$ Å at a resolution of $\lambda/\Delta\lambda \approx 1800$ and contains 2048 pixels (Stoughton et al. 2002).

As the templates provided by Bochanski et al. (2007) are normalized, two parameters determine the model m. These are the radial velocity and a multiplicative factor. Thus, if I let $t(\lambda, v)$ be the value of the template Doppler shifted by the velocity v at the wavelength λ, I have that

$m(\lambda) = a \cdot t(\lambda, v)$ where a is the multiplicative factor and v is the radial velocity. Thus,

$$\chi^2 = \sum_{i \in S} (\frac{f_i - a \cdot t(\lambda_i, v)}{\sigma_i})^2 \tag{2}$$

Basic calculus tells us that at the minimum of χ^2, both $\frac{\partial \chi^2}{\partial a} = 0$ and $\frac{\partial \chi^2}{\partial v} = 0$. From the first, it follows that the value of a at the minimum is given by

$$a = \frac{\sum_{i \in S} (\frac{f_i \cdot t(\lambda_i, v)}{\sigma_i^2})}{\sum_{i \in S} (\frac{t(\lambda_i, v)^2}{\sigma_i^2})} \tag{3}$$

As this is a function of v, I have reduced the problem of finding the minimum of χ^2 from a two dimensional problem to a one dimensional problem.

Let us now consider the nature of $t(\lambda, v)$. The templates created by Bochanski et al. (2007) give values for the flux at 0.1Å intervals from 3825Å to 9200Å. Thus, in order to determine the value of the flux at any wavelength other than at the exact values provided by the template, I must interpolate from the templates. I choose to use cubic spline interpolation for this purpose (Press et al. 1992). Thus, the value of $t(\lambda, v)$ can be determined by Doppler shifting the template by the velocity v and then interpolating to λ. Equivalently, it can be done by interpolating to the wavelength that results from Doppler shifting λ by $-v$. Since Doppler shifting λ by $-v$ gives the wavelength $\sqrt{\frac{1-\frac{v}{c}}{1+\frac{v}{c}}} \cdot \lambda$, $t(\lambda, v)$ is the result of interpolating the template to $\sqrt{\frac{1-\frac{v}{c}}{1+\frac{v}{c}}} \cdot \lambda$.

In the definition of χ^2 given in Equation 1, I took the sum to be over all pixels in S. While generally the sum would be taken over all the pixels, I exclude some pixels whose inclusion would severely impair the quality of the fit. A pixel is in S unless at least one of the following is true:

1. The wavelength of the pixel, λ, satisfies $\lambda > 9150$Å,

2. the wavelength of the pixel, λ, satisfies $6540\text{Å} < \lambda < 6585\text{Å}$, or

3. the BADSKYCHI mask bit was set for that pixel.

The reasons that I exclude these pixels are as follows. The templates provided by Bochanski et al. (2007) extend only to 9200Å, so clearly I can not use cubic spline interpolation to find the value of the flux at a wavelength greater than 9200Å. Since determining χ^2 requires interpolating the templates to the wavelength $\sqrt{\frac{1-\frac{v}{c}}{1+\frac{v}{c}}} \cdot \lambda$, this quantity must be less than 9200Å. While a sufficiently

large negative velocity will result in this quantity being greater than 9200Å for any λ, if I assume that $|v| \leq 1 \cdot 10^6 \frac{\mathrm{m}}{\mathrm{s}}$ (a reasonable assumption as it would be quite exceptional if any star was moving faster than $1 \cdot 10^6 \frac{\mathrm{m}}{\mathrm{s}}$), then for $\lambda < 9150$Å, $\sqrt{\frac{1-\frac{v}{c}}{1+\frac{v}{c}}} \cdot \lambda < 9200$Å. Thus, I exclude pixels with $\lambda > 9150$Å.

The strength of the Hα line varies significantly between M stars (Bochanski et al. 2007). Therefore, the strength of the line in the templates is not representative of all M stars. Thus, inclusion of the Hα would result in a worse fit. I remedy this by removing any pixels with wavelength $6540\text{Å} < \lambda < 6585\text{Å}$. This range was chosen as if I again assume that the speed of the star is less than $1 \cdot 10^6 \frac{\mathrm{m}}{\mathrm{s}}$, then the H$\alpha$ line (which has a wavelength of 6562.8Å) will fall within this range.

The BADSKYCHI mask bit indicates that the sky emission lines are not being well fit by the spectra extraction pipeline used by the SDSS. This is an issue as the light observed by the telescope is a combination of the stellar spectra and the sky emission lines so to determine the stellar spectra, the sky emission lines must be subtracted off from the observational data. If the spectra extraction pipeline does a poor job of fitting the sky emission lines, then this results in much greater errors in the resulting stellar spectrum. For this reason, I exclude pixels which have the BADSKYCHI mask bit set.

A full definition of χ^2 has now been given. While determining analytically what radial velocity yields the minimum χ^2 for a particular spectra and template is not feasible, doing so numerically is straightforward.

Once all eleven of the templates have been fit to each of the observations of a single object and the radial velocity that results in the minimum χ^2 has been determined for each pair of an observation and a template, I must determine which of the templates fit the object the best as obviously the object can only be one spectral type. If I let χ^2_{ij} represent the minimum χ^2 when the j$^{\text{th}}$ template is fit to the i$^{\text{th}}$ observation, then the template which best fits the object is that which corresponds to the value of j that gives the smallest value of $\sum_i \chi^2_{ij}$ where the sum is over all the observations. I then take the radial velocity values of the observations to be those determined by fitting it to that template. I then correct for the motion of the Earth by adding the barycentric

correction calculated by the SDSS pipeline to the calculated radial velocities.

2.2 Identifying Binaries

Once I have determined the radial velocity of each observation of each object, I now wish to determine from the radial velocities whether the object is undergoing RV variability. However, before doing this, I apply several cuts to the sample. I retain only observations that satisfy all of the following: the average signal to noise of the pixels is greater than 10, the observation is not among the 10% of observations with the greatest values of the χ^2 of the template fit, and after applying the two previous cuts, at least three observations of the object remain in the sample. After applying these cuts, 23,135 observations of 7,081 objects remain in the sample with 0 hr $\leq \Delta t \leq 4$ hr and 7,501 observations on 1,639 objects remain in the sample with 2 d $\leq \Delta t \leq 30$ d. Figure 1 shows the distributions of several properties of the stars that remain in the sample following these cuts.

Now for each of the remaining objects, if RV_i and $(\mathrm{S/N})_i$ represent the radial velocity after applying the barycentric correction and the average signal-to-noise ratio of all pixels of the i$^{\mathrm{th}}$ observation of the object, respectively, I compute

$$\Delta\mathrm{RV}_i = \mathrm{RV}_i - \frac{\sum_i \mathrm{RV}_i \cdot (\mathrm{S/N})_i}{\sum_i (\mathrm{S/N})_i} \tag{4}$$

for each observation of the object. This is the difference between the radial velocity of the observation and the weighted average of the radial velocities of all observations where the weight function is $(\mathrm{S/N})_i$.

Using the data from the sample with 0 hr $\leq \Delta t \leq 4$ hr, I must establish a means to identify an object as either an RV variable or not an RV variable. I do this as follows. For each object in the sample with 2 d $\leq \Delta t \leq 30$ d, I compute

$$x = \frac{\sum_{i=1}^{M} |\Delta\mathrm{RV}_i|}{M} \tag{5}$$

where M is the number of observations. I mark the object as a RV variable if the probability of obtaining a value of x greater than that of the object from a sample of observations that are not experiencing RV variations is less than 10^{-3}.

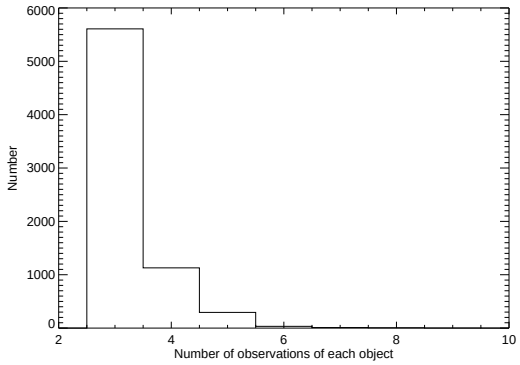

(a) A histogram of the number of observations of each object in the sample with 0 hr $\leq \Delta t \leq 4$ hr

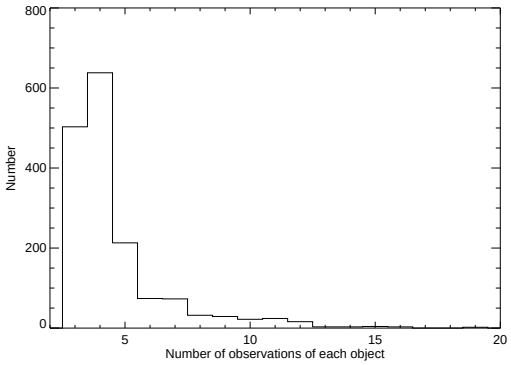

(b) A histogram of the number of observations of each object in the sample with 2 d $\leq \Delta t \leq 30$ d

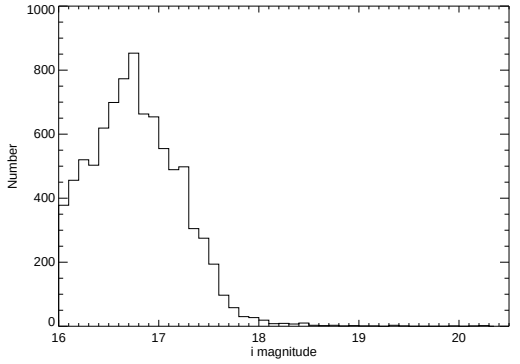

(c) A histogram of the i magnitude in the combined sample

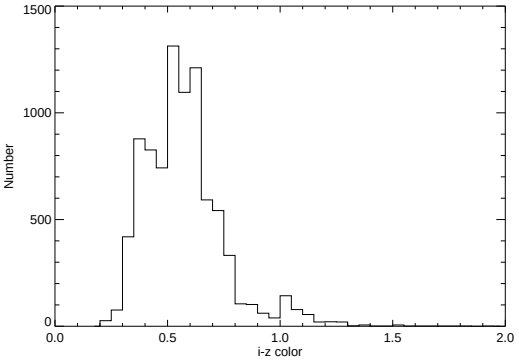

(d) A histogram of the $i - z$ color in the combined sample

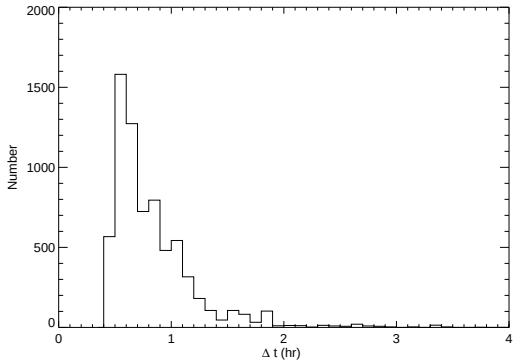

(e) A histogram of Δt in the sample with 0 hr $\leq \Delta t \leq 4$ hr

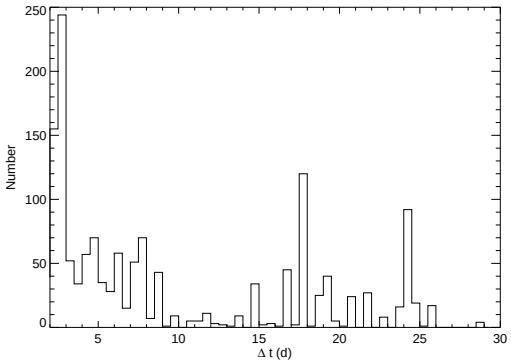

(f) A histogram of Δt in the sample with 2 d $\leq \Delta t \leq 30$ d

Figure 1: Histograms of several different properties of stars for the sample.

The sample of objects with 0 hr $\leq \Delta t \leq 4$ hr is a sample of observations that are not undergoing RV variations. As stated above, even if the object is a binary star and thus has RV variations, the change in the radial velocity in a period of 4 hours is small enough not to require consideration.

I run a Monte Carlo simulation of 10^7 hypothetical objects to determine a cutoff for x which is exceeded by only $10^7 \cdot 10^{-3} = 10^4$ of the simulated objects. For each trial, I choose the number of observations from the distribution of the number of observations of each object in the sample with 0 hr $\leq \Delta t \leq 4$ hr. I then choose the ΔRV value of each of these fake observations randomly from the values calculated for the objects in the sample with 0 hr $\leq \Delta t \leq 4$ hr and compute x using Equation 5. Once I have calculated x for each of the hypothetical objects, I then establish the cutoff value for x at a value so that exactly 10^4 of the simulated objects have a value of x greater than the cutoff. From this cutoff, I determine which stars from the sample with 2 d $\leq \Delta t \leq 30$ d are RV variables.

2.3 Bayesian Analysis

The key formula of Bayesian analysis is Bayes' theorem which states that

$$P(X|Y, I) \propto P(Y|X, I) \cdot P(X|I) \tag{6}$$

where $P(X|Y, I)$, the probability of X given Y and I, is the posterior distribution; $P(Y|X, I)$, the probability of Y given X and I, is the likelihood distribution; and $P(X|I)$, the probability of X given I, is the prior distribution for any X and Y where I is the relevant background information (Sivia & Skilling 2006). If I take $X_1, X_2, \ldots, X_n$ to be a set of hypotheses and Y to be the data and calculate the likelihood distribution and the prior distribution, I can then determine the posterior distribution from which I am able to determine which of the given hypotheses is most likely.

Let us now consider the specific problem I address here. Let D represent the number of objects detected, N represent a value for the close binary fraction, and B represent knowledge of any relevant background information about the objects and the observations of the objects such as the magnitudes of the objects in the u, g, r, i, and z bands, and the times of the observations. Now if I take $X = N$, $Y = D$ and $I = B$, then by Bayes' theorem

$$P(N|D, B) \propto P(D|N, B) \cdot P(N|B) \tag{7}$$

Let us now consider the likelihood function $P(D|N, B)$. As D represents the number of objects

detected as RV variables, it follows that

$$P(D|N,B) = \sum P(\{O_{i_1}, O_{i_2}, \ldots, O_{i_D}\}|N,B) \tag{8}$$

where $P(\{O_{i_1}, O_{i_2}, \ldots, O_{i_D}\}|N,B)$ is the probability that exactly the D objects, $i_1, i_2, \ldots, i_D$, are detected as RV variables and the sum is over all sets of D objects. Since whether or not one object is detected is independent of whether or not another object is detected,

$$P(\{O_{i_1}, O_{i_2}, \ldots, O_{i_D}\}|N,B) = \prod_{j \in L} P(O_j|N,B) \cdot \prod_{j \notin L} P(\bar{O}_j|N,B) \tag{9}$$

where $L = \{i_1, i_2, \ldots, i_D\}$, $P(O_j|N,B)$ is the probability the j$^{\text{th}}$ object is detected and $P(\bar{O}_j|N,B)$ is the probability the j$^{\text{th}}$ object is not detected. Substituting that into Equation 8 gives

$$P(D|N,B) = \sum [\prod_{j \in L} P(O_j|N,B) \cdot \prod_{j \notin L} P(\bar{O}_j|N,B)] \tag{10}$$

I now must consider how to calculate $P(O_j|N,B)$ and $P(\bar{O}_j|N,B)$. Following Maxted & Jeffries (2005) in assuming that the only cause of RV variability is binary stars, it follows that the probability that the j$^{\text{th}}$ object is detected as an RV variable is $Np_{detect,j} + (1-N) \cdot 10^{-3}$ where $p_{detect,j}$ gives the probability that I will detect the j$^{\text{th}}$ object as an RV variable if it is in fact a binary star. Note that the term $(1-N) \cdot 10^{-3}$ arises from the fact that $1-N$ is the probability that the object is not a binary star while 10^{-3} is the probability that an object will be detected as an RV variable if it is not a binary star by the definition of the criterion I established to determine whether or not an object is an RV variable. Thus, $P(O_j|N,B) = Np_{detect,j} + (1-N) \cdot 10^{-3}$ and $P(\bar{O}_j|N,B) = 1 - P(O_j|N,B) = 1 - [Np_{detect,j} + (1-N) \cdot 10^{-3}]$. I now must determine $p_{detect,j}$ for each of the objects in the sample with $2 \text{ d} \leq \Delta t \leq 30$ d. I shall do this using a Monte Carlo simulation.

I ran a Monte Carlo simulation of 10^5 virtual binary stars for each of the 1,639 objects in the sample with $2 \text{ d} \leq \Delta t \leq 30$ d to see what fraction would be identified as RV variables using the above methods to identify RV variables. In order to do this, I must specify distributions for the various properties of a binary system. I use the following distributions.

Semimajor axis, a: In order to have a reasonable chance to detect a binary in the sample with $2 \text{ d} \leq \Delta t \leq 30$ d, Δt must be a significant fraction of the period of the system. If I assume

that it is necessary for us to see at least $\frac{1}{3}$ of the orbit to have a possibility of detecting the object, it follows that $P < 3 \cdot 2592000$ s $= 7776000$ s. Since the stars I am looking at are M stars, $m_1 < 0.5\ M_\odot$, so it then follows from Kepler's third law that $a < 0.40$ AU. Thus, $a < 0.40$ AU is necessary for there to be a reasonable chance of detecting the binary. The distribution of the semimajor axis for systems with such small semimajor axes is not known. I shall consider two different distributions. The first is a uniform distribution from 0.01 to 0.4 AU, while the second distribution is a linear distribution such that $P(a) \propto a$ that also runs from 0.01 to 0.4 AU. The lower limit of $.01$ AU is chosen as systems with smaller semimajor axes would be incredibly uncommon. Note that one would expect the uniform distribution to overestimate the value of $p_{detect,j}$ as the the correct distribution should have a higher probability of larger separations and a corresponding lower probability of smaller separations (Allen 2007). This overestimate of $p_{detect,j}$ in turn implies that the best fit binary fraction N will be underestimated.

Mass ratio, q: I follow Allen (2007) in using a power law distribution with a minimum of $q = 0.02$. Thus, if I let γ represent the power law index, the probability distribution function of q is

$$P(q) = \frac{q^\gamma}{\int_{.02}^{1} q^\gamma \, \mathrm{d}q} \tag{11}$$

for $.02 < q < 1$ and $P(q) = 0$ for $0 < q < .02$. I test distributions that use three different values for γ. I test $\gamma = 1.8$, the value that Allen (2007) found and $\gamma = 1.2$ and 2.2, the extreme values on the 1σ confidence interval given by Allen (2007).

Primary mass, m_1: Unfortunately, there is not a good way to determine the mass of the primary from the observed spectra as there are no well-calibrated mass-color or mass-luminosity relationships using the SDSS filters. Additionally, not knowing the metallicity or age of the star increases the uncertainty in determining the mass of the star. However, I am able to obtain a rudimentary estimate of the primary mass by the following means. Using the color transformations provided by Davenport et al. (2006), from my knowledge of the apparent magnitude of the star in the r and i bands, I can determine the $i - J$ color. Also, using the color-magnitude relationships provided by West, Walkowicz, & Hawley (2005), I can determine the absolute magnitude, M_i, in

the i band from the $i-z$ color of the objects. Then, since $i-J=M_i-M_J$, I can calculate M_J. Finally, the mass-luminosity relations of Delfosse et al. (2000) allow for the determination of the star's mass from M_J. While the individual values of the mass obtained by these means are highly questionable, this is remedied by choosing the primary mass from a uniform distribution from .75 to 1.25 times the calculated mass and by the fact that I am using this mass value for a Monte Carlo simulation.

Eccentricity, e: It is well known that binaries with very short periods (P< 10d) are highly likely to undergo tidal circularization (Duquennoy & Mayor 1991, Meibom & Mathieu 2005) and thus have circular orbits. While those objects in the simulation with the largest separations can possibly have $e \neq 0$, I shall not take this into account here. Thus, I assume that $e=0$ for all objects.

Orbital phase, f: The orbital phase at the time of the first observation must be chosen from a uniform distribution from 0 to 1.

Inclination, i: The inclination must be chosen from a uniform distribution from 0 to π radians.

Longitude of periastron, ω: The longitude of periastron must be chosen from a uniform distribution from 0 to 2π radians.

For each trial, I randomly choose values for the above properties of the system from the given distributions. I then consider the same number of observations as there were of the actual object, with the same time separation between the observations. Then, for each observation, I can calculate the hypothetical radial velocity using the formula

$$RV = \frac{2\pi a \sin i}{P(1-e^2)^{1/2}}[cos(\theta+\omega)+e\cos\omega] \tag{12}$$

where the true anomaly, θ, satisfies $\cos\theta = \frac{\cos E - e}{1-e\cos E}$, the eccentric anomaly, E, is given by $E - e\sin E = \frac{2\pi}{P}(t-T)$, and T is the time of periastron passage (Hilditch 2001). While I do not know T, I do know that $\frac{2\pi}{P}(t-T) = \frac{2\pi}{P}(t-t_1) + \frac{2\pi}{P}(t_1-T) = \frac{2\pi}{P}(t-t_1) + 2\pi f$ where t_1 is the time of the first observation and the second equality is true because $\frac{t_1-T}{P}$ is simply the orbital phase, f. I then calculate the value of ΔRV for each observation using the values of S/N for each observation of the actual object. I then must include the error that occurs in the measurement of the RV from the spectra by adding a number randomly chosen from the ΔRV values for the sample

with 0 hr $\leq \Delta t \leq 4$ hr to the calculated ΔRV. I can then compute x using Equation 5 just as I did for the sample with 2 d $\leq \Delta t \leq 30$ d. If the value of x is greater than the cutoff value determined in section 2.2, 11.9 km/s, then this star would have been detected. By running 10^5 trials for each of the 1,639 objects in our sample with 2 d $\leq \Delta t \leq 30$ d and determining the fraction of trials in which we detect the simulated object, I have determined $p_{detect,j}$ and am thus able to determine $P(D|N,B)$.

I now must specify the prior distribution, $P(N|B)$. I follow Allen (2007) in choosing a prior that assumes no prior knowledge and therefore is not biased towards any particular values of N. Thus, as N is a scale parameter, the proper prior to use is the Jeffreys' prior (Sivia & Skilling 2006),

$$P(N|B) \propto \frac{1}{N}. \tag{13}$$

I have now specified both the likelihood and prior distribution. Thus, by simply multiplying the two, I have the posterior distribution. The posterior distribution is

$$P(N|D,B) \propto P(D|N,B) \cdot P(N|B) \tag{14}$$

$$\propto \sum [\prod_{j \in L} P(O_j|N,B) \cdot \prod_{j \notin L} P(\bar{O}_j|N,B)] \cdot \frac{1}{N} \tag{15}$$

$$\propto \sum [\prod_{j \in L} [N p_{detect,j} + (1-N)10^{-3}] \cdot \prod_{j \notin L} [N p_{detect,j} + (1-N)10^{-3}]] \cdot \frac{1}{N} \tag{16}$$

I can then determine the constant of proportionality using the normalization condition

$$\int_0^1 P(N|D,B)\,\mathrm{d}N = 1. \tag{17}$$

From the posterior distribution, I am able to determine the best fit value of the binary fraction and uncertainties in this value.

3 Results

A histogram of the values of ΔRV computed for the sample with 0 hr $\leq \Delta t \leq 4$ hr in section 2.2 is shown in Figure 2. The standard deviation of the ΔRV values is 4.1 km/s which compares favorably with the rms velocity error of 5.5 km/s at $g = 18.5$ and 12 km/s at $g = 19.5$ reported by Abazajian et al. (2009). However, it is interesting to note that there is a small set of objects

with very large ΔRV values. Among the 7081 objects in the sample with 0 hr $\leq \Delta t \leq 4$ hr, 15 of the objects have at least one observation for which the value of $\Delta RV > 20$ km/s. This is far greater than would be expected if the values of ΔRV followed a Gaussian distribution as one would expect. These objects certainly deserve further consideration and possibly further observation.

Figure 2: A histogram of the ΔRV for the sample with 0 hr $\leq \Delta t \leq 4$ hr

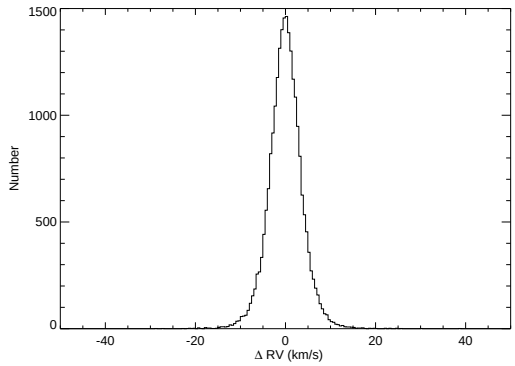

Table 1: $\langle p_{detect,j} \rangle$ and the best fit value of N and the 1σ (68.3%) confidence interval on N for each combination of a and q distribution

P(a)	P(q)	$\langle p_{detect,j} \rangle$	N
Uniform	$\gamma = 1.2$	0.38	$3.1^{+0.7}_{-0.8}\%$
Uniform	$\gamma = 1.8$	0.39	$3.1^{+0.6}_{-0.9}\%$
Uniform	$\gamma = 2.2$	0.39	$3.0^{+0.6}_{-0.9}\%$
Linear	$\gamma = 1.2$	0.27	$4.3^{+0.9}_{-1.2}\%$
Linear	$\gamma = 1.8$	0.28	$4.2^{+0.9}_{-1.1}\%$
Linear	$\gamma = 2.2$	0.29	$4.1^{+0.8}_{-1.2}\%$

Following the procedure given in section 2.2, I determined the cutoff for x to be 11.9 km/s. Among the 1639 objects in the sample with 2 d $\leq \Delta t \leq 30$ d, 22 exceed this cutoff and were detected as RV variables.

The data produced by section 2.2 and the models for the orbital parameters were fed into the Monte Carlo simulation which in turn feeds the calculated values of $p_{detect,j}$ into Equation 16. The resulting posterior distribution is shown in Figure 3 for each combination of a and q distribution. Table 1 gives the average value of $p_{detect,j}$ over all the objects and the best fit value of N and the 1σ confidence interval on N for each combination of a and q distribution. From Table 1, it is clear that changing the power law index, γ has negligible impact on N. However, using a linear distribution

for a as opposed to a uniform distribution increases N as I expected, due to the decrease of $p_{detect,j}$ that results from using a distribution with a higher probability of large separations and a lower probability of small separations. The increase in N that results from using a linear distribution instead of a uniform distribution is 1.1%. From here forth, I shall focus on the value of N derived for a uniform distribution. Thus, the close binary fraction of the objects in my sample is $3.1^{+0.6}_{-0.9}\%$.

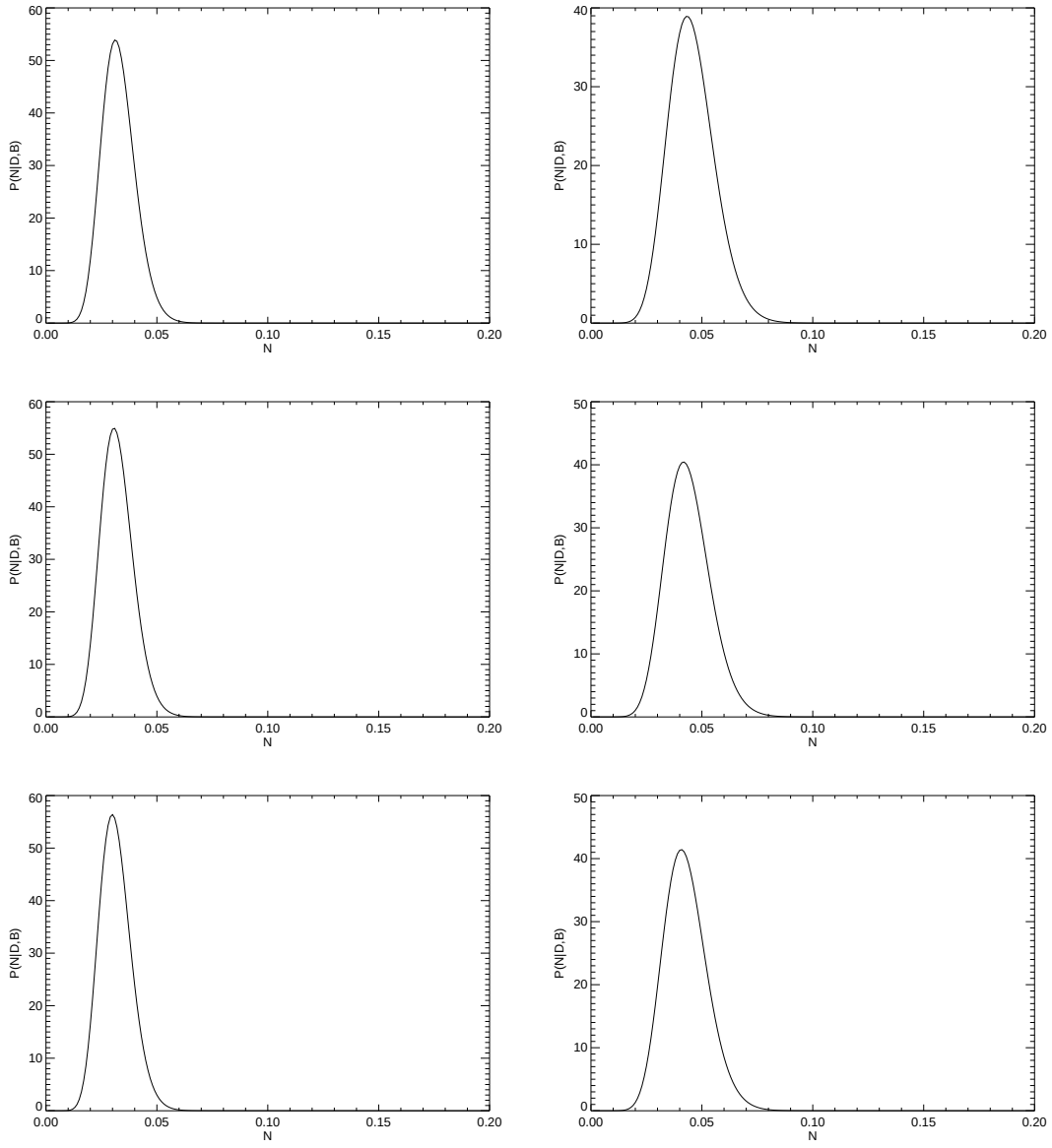

Figure 3: The left column is for a uniform distribution of a and the right column is for a linear distribution of a. The rows are for $\gamma = 1.2$, 1.8, and 2.2, respectively

4 Discussion

Other investigations have determined the close binary fraction for various spectral types. Duquennoy & Mayor (1991) found that 5.6% of G stars are binaries with $a < 0.4$ AU, while Blake et al. (2010) found that 2.5% of late-M and L stars are binaries with $a < 1.0$ AU. Figure 4 summarizes these results. Note that the value given by Blake et al. (2010) must significantly overestimate for the fraction of late-M and L stars which are binaries with $a < 0.4$ AU as it also includes binaries with 0.4 AU $< a < 1.0$ AU. It is thus apparent that the close binary fraction decreases with decreasing primary mass. While others have noted that the total binary fraction decreases with decreasing primary mass, it has not been previously shown that the same holds for the close binary fraction.

Figure 4: The values for the close binary fraction determined by Duquennoy & Mayor (1991), Blake et al. (2010), and this paper as a function of mass. The error bounds on my value give the 1σ uncertainty in the close binary fraction that I found. Error bounds are not available for the value given by Duquennoy & Mayor (1991) and as I am using the value provided by Blake et al. (2010) as an upper limit, an error bound is not applicable.

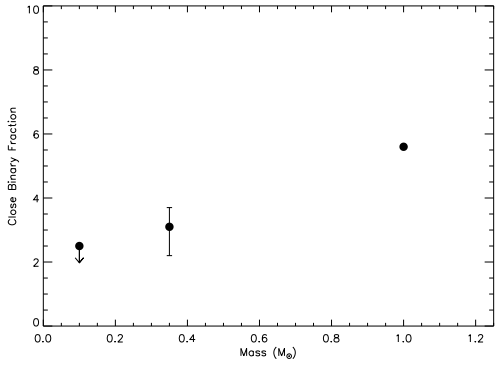

The current understanding of star formation is that stars form in small-N clusters, multiple systems containing $N \geq 3$ stars, which are then broken apart by two processes, dynamical decay and dynamical destruction (Goodwin et al. 2007). In dynamical decay, due to the instability of multiple systems, a member of the system is ejected on a relatively short time scale. Anosova (1986) showed that in the vast majority of cases, the star ejected is the least massive of the stars in the system. In dynamical destruction, interactions with other stars in the star cluster disrupt binary stars; however, this occurs on a far longer time scale than dynamical decay (Goodwin et al.

2007). Note that the previously observed correlation between mass and the total binary fraction supports both of these theories. Due to the preferential ejection of lower mass stars from systems by dynamical decay, it follows that one would expect a low mass star to have a higher fraction of single stars and a corresponding lower fraction of binary stars while low mass star binaries would also be more likely to undergo dynamical disruption due to interactions with more massive stars in the star cluster which also leads to a lower binary fraction.

However, if I consider the previous results that the total binary fraction is lower for lower mass stars and that the peak of the semimajor axis distribution is at a lower values of a for lower mass stars (Duquennoy & Mayor 1991, Fischer & Marcy 1992, Allen 2007) along with my result here that the close binary fraction is lower for low mass stars, I am then able to conclude that dynamical destruction alone cannot account for the observations and dynamical decay or some other process must play an important role in star formation. Heggie (1975) and Hills (1975) found that while dynamical destruction disrupts loosely bound binaries, it actually results in close binaries such as those that I considered here to become even more tightly bound. Therefore, if dynamical destruction is the only process governing star formation, then it follows that the close binary fraction should be constant as a function of mass. This contradicts the result that I obtained here that the close binary fraction is smaller for low mass stars than for more massive stars. Thus, it follows that some process other than dynamical destruction serves an important role in star formation. This could be dynamical decay or some other yet unknown process.

Fischer & Marcy (1992) also determined the close binary fraction for $a < 0.4$ AU. In their sample of 62 objects, they detected 1 object and after correcting for their detection efficiency, found the close binary fraction to be $1.8^{+1.8}_{-1.8}\%$. Clearly, a sample that includes only one detection results in a very imprecise determination of the close binary fraction, but it is worth noting that my results agree with those of Fischer & Marcy (1992) to within their error.

This analysis is distinct from previous works on the binary fraction in the sample that I consider. Previous works such as Duquennoy & Mayor (1991), Fischer & Marcy (1992), and Blake et al. (2010) have considered small samples in which each object was observed a large number of times

with instruments capable of very high radial velocity precision. Here I consider a far larger sample with a lower number of observations per object that was observed at significantly lower precision. Despite this limitation, I still was able to obtain interesting results. This suggests that, in the future, large scale surveys such as the SDSS can be used in the place of samples observed specifically to determine the binary fraction.

5 Conclusions and Future Work

I have determined the close binary fraction ($a < 0.4$ AU) of M stars to be $3.1^{+0.6}_{-0.9}\%$. By comparing this result to the close binary fraction of G stars and ultracool dwarfs (late-M and L dwarfs), I have shown that the close binary fraction is a decreasing function of mass. While it has previously been shown that the total binary fraction is a decreasing function of mass, this result had not previously been shown for the close binary fraction.

It would be intriguing to observe both the 22 objects in the sample with 2 d $\leq \Delta t \leq 30$ d that I found to be binary stars and the 15 stars in the sample with 0 hr $\leq \Delta t \leq 4$ hr that I found to have very large ΔRV values. Tables 2(a) and 2(b) give the right ascension, declination, i magnitude, and the value of x computed using Equation 5 for the 22 detected binaries and the 15 objects with abnormally large ΔRV values, respectively. It would also be valuable to conduct a meta-analysis of this data set together with the data sets provided by Blake et al. (2010) and Allen (2007). This would allow me to determine the binary fraction for a larger range of a.

Future large scale spectroscopic surveys that provide more precise data than that of the SDSS will allow for more accurate determinations of the close binary fractions and will allow for the extension of this method to binaries with separations larger than $a = 0.4$ AU. Additionally, the close binary fraction of stars of later spectral types remains relatively poorly constrained. A large sample of more precise data would allow for an analysis similar to that conducted here to be carried out on L stars.

Table 2: The left and right subtables give the right ascension, declination, i magnitude, and the value of x calculated using Equation 5 for each object in the sample with 2 d $\leq \Delta t \leq$ 30 d that I detected as a binary and the objects in the sample with 0 hr $\leq \Delta t \leq$ 4 hr for which $\Delta RV >$ 20 km/s, respectively.

RA	DEC	i	x
312.19107	0.667030	17.47	47115.1
343.70959	-10.167570	17.17	17300.3
248.06541	0.988510	16.66	24150.0
127.61649	45.793491	17.33	13447.2
175.21191	53.384460	16.65	12511.2
17.66198	-1.235980	17.31	12088.3
17.72551	0.874290	16.54	14004.6
5.34449	-0.886580	17.07	13678.3
248.50588	0.836120	16.87	14091.3
321.44168	-6.149620	16.12	16083.4
5.61987	-1.135260	16.59	12455.9
11.94934	-0.764040	17.02	16743.2
116.11788	19.265209	17.47	70133.7
116.69219	28.441660	17.55	11926.7
184.93391	26.133289	16.13	12320.1
175.12529	15.708770	16.18	47315.8
4.69498	0.043800	17.41	20002.2
162.62589	42.247631	16.44	23621.8
164.31570	43.162769	16.33	23955.8
332.20187	0.069430	17.12	23225.4
177.85146	37.331612	16.37	13815.2
132.17156	23.347710	16.34	91953.5

RA	DEC	i	x
34.659969	0.829670	16.98	16232.7
127.13995	34.258789	16.79	14789.3
134.84064	37.196651	18.19	15016.6
118.18209	25.824551	17.39	15240.2
237.20148	36.467701	17.04	16921.6
7.93530	0.509350	17.49	13935.1
248.93524	24.508989	16.78	13007.9
248.48320	29.623631	16.98	12527.1
193.78691	32.147221	17.04	9684.0
247.58414	30.881821	16.62	19982.4
218.85271	23.380430	16.97	16687.1
169.19923	29.767429	16.24	14342.1
111.67760	41.712002	16.64	14201.5
172.48730	31.313780	16.78	83841.9
140.93979	22.409000	16.56	47684.3

References

[1] Abazajian, K. N., et al. 2009, ApJS, 182, 543

[2] Allen, P. R. 2007, ApJ, 668, 492

[3] Anosova, J. P. 1986, Ap&SS, 124, 217

[4] Bochanski, J. J., West, A. A., Hawley, S. L., & Covey, K. R. 2007, AJ, 133, 531

[5] Blake, C. H., Charbonneau, D., & White, R. J. 2010, arXiv:1008.3874

[6] Davenport, J. R. A., West, A. A., Matthiesen, C. K., Schmieding, M., & Kobelski, A. 2006, PASP, 118, 1679

[7] Delfosse, X., Forveille, T., Ségransan, D., Beuzit, J.-L., Udry, S., Perrier, C., & Mayor, M. 2000, A&A, 364, 217

[8] Duquennoy, A., & Mayor, M. 1991, A&A, 248, 485

[9] Fischer, D. A., & Marcy, G. W. 1992, ApJ, 396, 178

[10] Goodwin, S. P., Kroupa, P., Goodman, A., & Burkert, A. 2007, Protostars and Planets V, 133

[11] Heggie, D. C. 1975, MNRAS, 173, 729

[12] Hilditch, R. W. 2001, An Introduction to Close Binary Stars, Cambridge University Press

[13] Hills, J. G. 1975, AJ, 80, 809

[14] Knapp, G. et al. 2010 (in prep.)

[15] Maxted, P. F. L., & Jeffries, R. D. 2005, MNRAS, 362, L45

[16] Meibom, S., & Mathieu, R. D. 2005, ApJ, 620, 970

[17] Press, W. H., Teukolsky, S. A., Vetterling , W. T., Flannery, B. P. 1992, Numerical Recipes: The Art of Scientific Computing. 2nd ed. Cambridge University Press

[18] Sivia, D. S. & Skilling, J. 2006, Data Analysis, Clarendon Press Oxford

[19] Stoughton, C., et al. 2002, AJ, 123, 485

[20] West, A. A., Walkowicz, L. M., & Hawley, S. L. 2005, PASP, 117, 706